Electronic Supplementary Material (ESI) for Inorganic Chemistry Frontiers.

Electronic Supplementary Information

Dynamic covalent bonding for directed construction of molecular cages toward carbon dioxide reduction

Jingting He, [†a] Man Dong, [†b] Yang Zhao, [b] Dongxu Cui, [b] Xiaohui Yao, [b] Fanfei Meng, [a] Wei Li, [b] Shuai Yang, [b] Chunyi Sun,[*b] and Zhongmin Su[*a]

[a]School of Materials Science and Engineering, Changchun University of Science and Technology, Changchun, 130022 Jilin, China. E-mail: zmsu@nenu.edu.cn

[b]Key Laboratory of Polyoxometalate Science of Ministry of Education, Northeast Normal University, Changchun, 130024 Jilin, China. E-mail: suncy009@nenu.edu.cn

[*]Corresponding author: e-mail: zmsu@nenu.edu.cn; suncy009@nenu.edu.cn

Table S1 Crystallographic data of Zr-CHO and Schiff-base ZrOC-1

Compound	Zr-CHO	Schiff-base ZrOC-1
Empirical formula	$C_{43}H_{40}ClO_{14}Zr_3$	$C_{78}H_{66}Cl_2N_6O_{22}Zr_6$
Formula weight	1089.86	2057.58
Crystal system	triclinic	monoclinic
Space group	P-1	C2/c
Temperature (K)	293(2)	173
Wavelength (Å)		
a (Å)	10.4744(4)	45.504(9)
b (Å)	10.9063(4)	17.800(3)
c (Å)	21.5947(8)	15.373(3)
α (°)	83.359(2)	90
γ (°)	72.183(2)	90
Volume ($Å^{3)}$	2331.37(15)	12265(4)
Z	2	4
ρcalc g/cm^3	1.553	1.114
μ/mm^{-1}	6.459	4.861
F (000)	1094	4104
2Θ range (°)	4.122 to 125.276	5.342 to 76.16
Reflections collected	56280	25401
Independent reflections	7324 [R_{int}= 0.0608, R_{sigma}= 0.0435]	3250[R_{int}=0.0983, R_{sigma}= 0.0608]
Goodness-of-fit on F^2	1.077	1.053
Final R indexes [I>=2σ (I)]	R_1= 0.0667, wR_2= 0.1729	R_1= 0.1154, wR_2= 0.2962
Final R indexes [all data]	R_1= 0.0900, wR_2= 0.1879	R_1= 0.1364, wR_2= 0.3153

[a]$R_1 = \Sigma||Fo|-|Fc||/\Sigma|Fo|$; [b]$wR_2 = \{\Sigma [w(Fo^2-Fc^2)^2]/\Sigma [w(Fo^2)^2]\}^{1/2}$

Table S2 Bond length of Zr-CHO

Atom	Atom	Length/A°	Atom	Atom	Length/A°
Zr01	Zr02	3.3407(10)	C00I	C00J	1.488(13)
Zr01	Zr03	3.3508(10)	C00J	C00Q	1.369(16)
Zr01	O005	2.123(5)	C00J	C00V	1.393(16)
Zr01	O006	2.077(5)	C00K	C00O	1.380(15)
Zr01	O007	2.121(5)	C00K	C00S	1.419(15)
Zr01	O008	2.173(6)	C00L	C00T	1.390(17)
Zr01	O00A	2.208(6)	C00L	C017	1.392(17)
Zr01	C00K	2.534(10)	C00M	C01E	1.511(19)
Zr01	C00O	2.526(10)	C00O	C00U	1.368(15)
Zr01	C00R	2.555(10)	C00Q	C019	1.363(15)
Zr01	C00S	2.525(10)	C00R	C00S	1.383(15)
Zr01	C00U	2.530(10)	C00R	C00U	1.359(15)
Zr02	Zr03	3.3466(11)	C00T	C01B	1.387(16)
Zr02	O006	2.063(5)	C00V	C015	1.376(15)
Zr02	O007	2.115(5)	C00W	C010	1.375(18)
Zr02	O009	2.126(6)	C00W	C012	1.358(18)
Zr02	O00C	2.190(6)	C00Y	C00Z	1.353(18)
Zr02	O00D	2.220(6)	C00Y	C012	1.333(17)
Zr02	C013	2.523(13)	C00Z	C010	1.455(18)
Zr02	C014	2.517(11)	C011	C015	1.380(17)
Zr02	C016	2.543(12)	C011	C019	1.350(17)
Zr02	C018	2.532(12)	C011	C01F	1.534(13)
Zr02	C01C	2.530(13)	C013	C014	1.37(2)
Zr03	O005	2.127(5)	C013	C01C	1.34(2)
Zr03	O006	2.075(5)	C014	C018	1.43(2)
Zr03	O009	2.113(6)	C016	C018	1.359(19)
Zr03	O00B	2.194(6)	C016	C01C	1.28(2)
Zr03	O00E	2.208(6)	C017	C01D	1.378(16)
Zr03	C00W	2.530(11)	C01A	C01B	1.336(19)
Zr03	C00Y	2.531(11)	C01A	C01D	1.390(19)
Zr03	C00Z	2.517(11)	C01A	C01M	1.518(17)
Zr03	C010	2.526(12)	C01E	C01G	1.41(2)
Zr03	C012	2.541(11)	C01E	C01J	1.49(3)
O008	C00H	1.263(13)	C01F	O01K	1.214(14)
O00A	C00I	1.261(12)	C01F	O2	1.222(16)
O00B	C00I	1.262(12)	C01G	C01N	1.41(2)
O00C	C00M	1.261(16)	O01H	C01M	1.21(3)
O00D	C00H	1.255(12)	C01I	C01L	1.33(2)
O00E	C00M	1.242(16)	C01I	C01N	1.38(2)
C00F	C00N	1.300(13)	C01I	C9	1.549(14)
C00F	C00P	1.439(13)	C01J	C01L	1.45(2)
C00F	C00X	1.423(13)	C01M	O11	1.241(18)

O00G	C00N	1.248(12)	O3	C9	1.197(13)
C00H	C00L	1.486(14)	C9	O40	1.168(16)

Table S3 Bond length of Schiff-base ZrOC-1

Atom	Atom	Length/A°	Atom	Atom	Length/A°
Zr1	Zr2	3.356(4)	N2	C19	1.214(10)
Zr1	Zr3	3.359(4)	N3	C29	1.28(3)
Zr1	O1	2.10(2)	C0AA	C17	1.456(14)
Zr1	O3	2.05(2)	C2AA	C3	1.455(19)
Zr1	O4	2.108(19)	C6	C26	1.31(4)
Zr1	O71	2.25(2)	C6	C28	1.32(4)
Zr1	O9	2.274(18)	C7	C9	1.35(4)
Zr1	C7	2.50(3)	C7	C18	1.39(4)
Zr1	C8	2.58(3)	C8	C18	1.35(4)
Zr1	C9	2.50(3)	C8	C37	1.34(4)
Zr1	C18	2.53(3)	C9	C37	1.39(4)
Zr1	C37	2.54(3)	C10	C12	1.43(4)
Zr2	Zr3	3.351(4)	C10	C26	1.39(4)
Zr2	O21	2.18(2)	C12	C28	1.34(4)
Zr2	O3	2.07(2)	C14	C20	1.42(4)
Zr2	O4	2.140(19)	C14	C30	1.36(4)
Zr2	O8	2.14(2)	C15	C31	1.39
Zr2	O11	2.10(2)	C15	C35	1.39
Zr2	C6	2.49(3)	C31	C2	1.39
Zr2	C10	2.50(3)	C31	C19	1.444(9)
Zr2	C12	2.51(3)	C2	C33	1.39
Zr2	C26	2.53(3)	C33	C17	1.39
Zr2	C28	2.55(3)	C17	C35	1.39
Zr3	O1	2.120(19)	C16	C20	1.36(4)
Zr3	O3	2.10(2)	C16	C24	1.42(4)
Zr3	O6	2.21(2)	C21	C1AA	1.39
Zr3	O10	2.225(18)	C21	C13	1.39
Zr3	O11	2.12(2)	C21	C27	1.465(19)
Zr3	C14	2.54(3)	C1AA	C23	1.39
Zr3	C16	2.51(3)	C23	C3	1.39
Zr3	C20	2.51(3)	C3	C25	1.39
Zr3	C24	2.49(3)	C25	C13	1.39
Zr3	C30	2.53(3)	C22	C38	1.470(19)
O2	C22	1.252(16)	C24	C30	1.39(4)
O6	C2AA	1.265(16)	C29	C32	1.465(19)
O7	C22	1.249(16)	C32	C34	1.39
O8	C2AA	1.247(16)	C32	C5	1.39
O9	C0AA	1.257(16)	C34	C36	1.39
O10	C0AA	1.241(16)	C36	C38	1.39
N1	N3	1.40(3)	C38	C39	1.39
N1	C27	1.21(3)	C39	C5	1.39
N2	N21	1.460(11)			

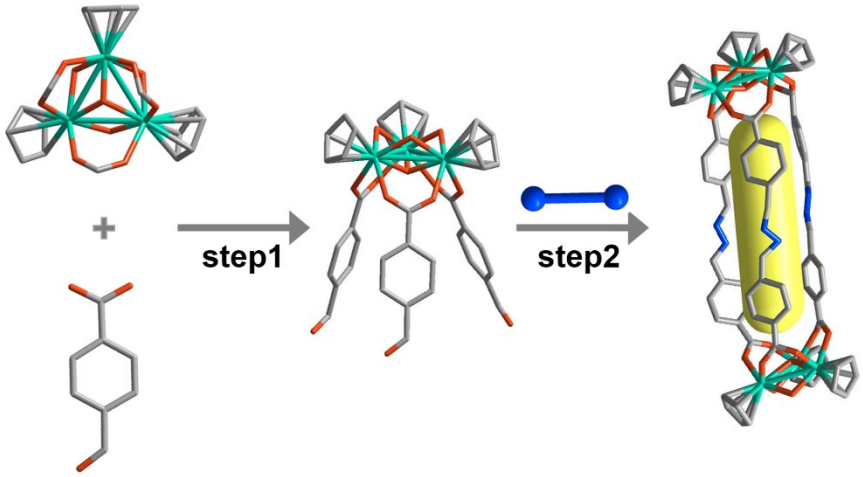

Fig. S1. Schematic illustration on synthetic strategy of Schiff-base ZrOC-1.

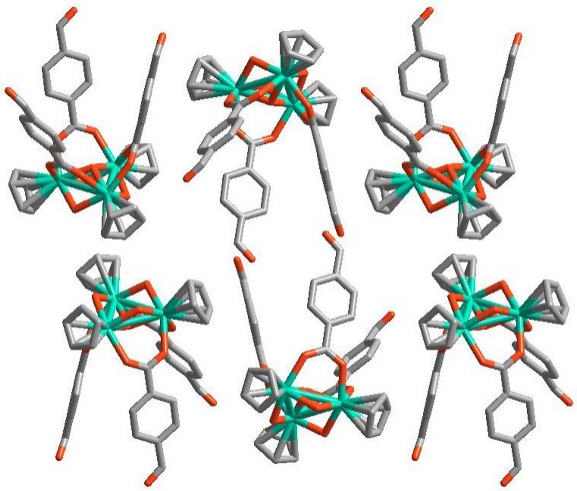

Fig. S2. The packing view of Zr-CHO along the a-axis. Color codes: blue-green Zr; black C; red O.

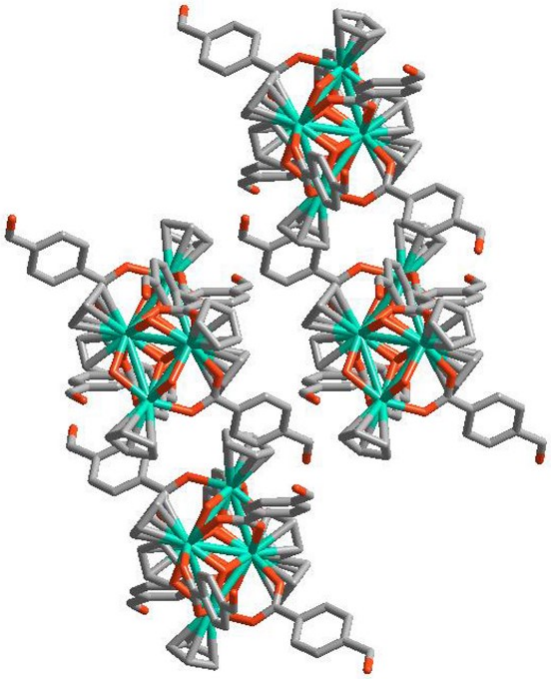

Fig. S3. The packing view of Zr-CHO along the b-axis. Color codes: blue-green Zr; black C; red O.

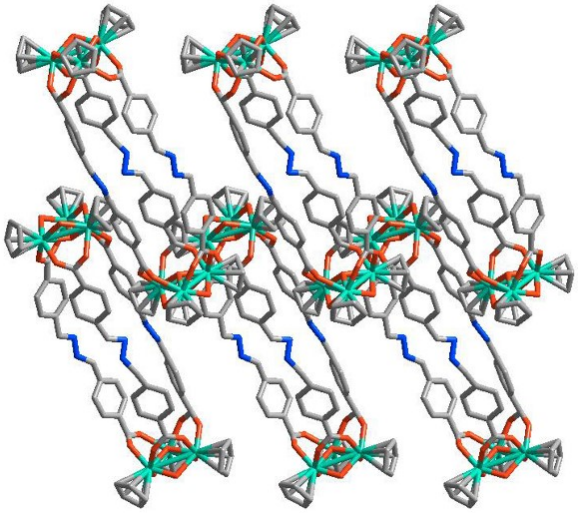

Fig. S4. The packing view of Schiff-base ZrOC-1 along the b-axis. Color codes: blue-green Zr; blue N; black C; red O.

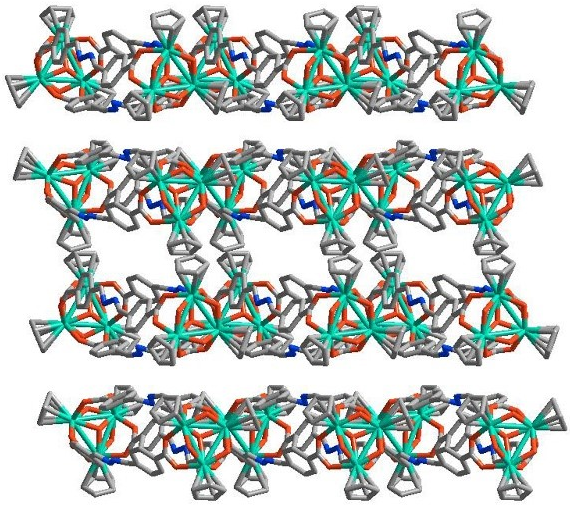

Fig. S5. The packing view of Schiff-base ZrOC-1 along the c-axis. Color codes: blue-green Zr; blue N; black C; red O.

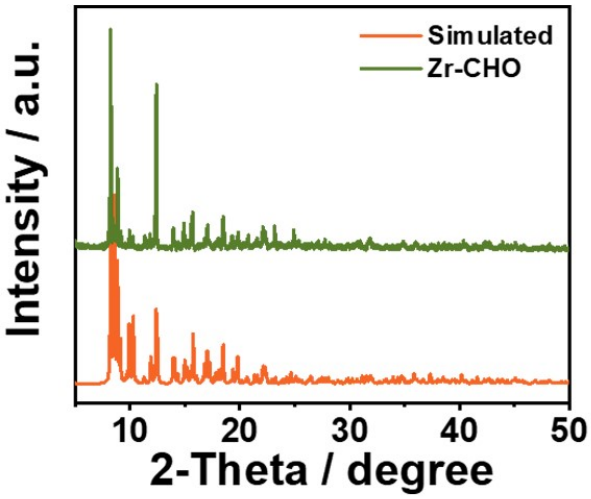

Fig. S6. XRD pattern of Zr-CHO.

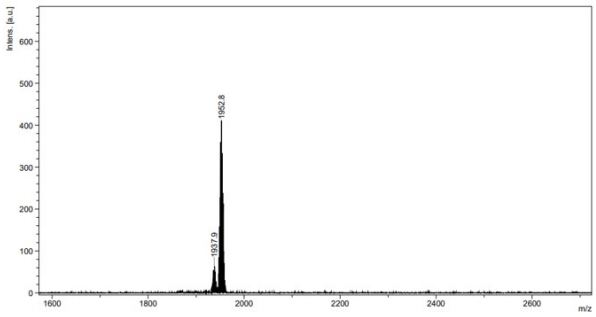

Fig. S7. The MS of Schiff-base ZrOC-1.

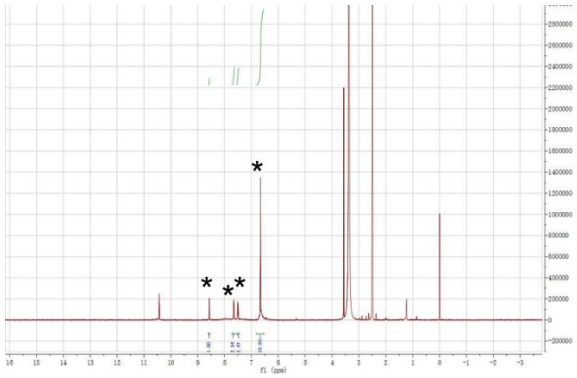

Fig. S8. ^{1}H NMR spectrum of Schiff-base ZrOC-1.

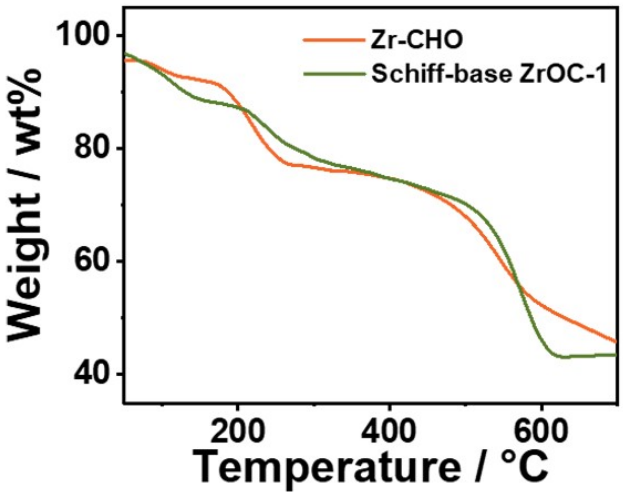

Fig. S9. TGA of Zr-CHO and Schiff-base ZrOC-1.

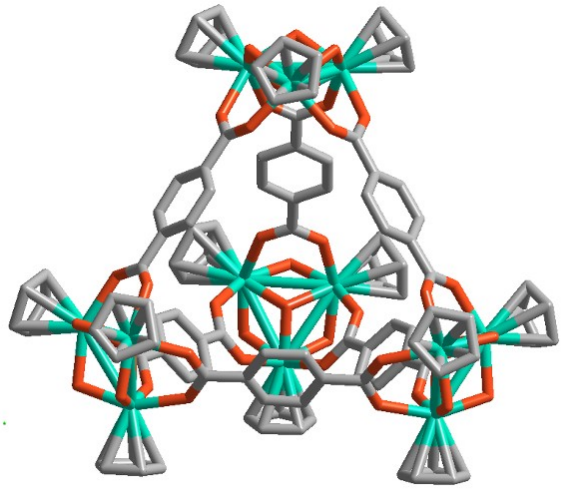

Fig. S10. The cage structure of ZrT-1.

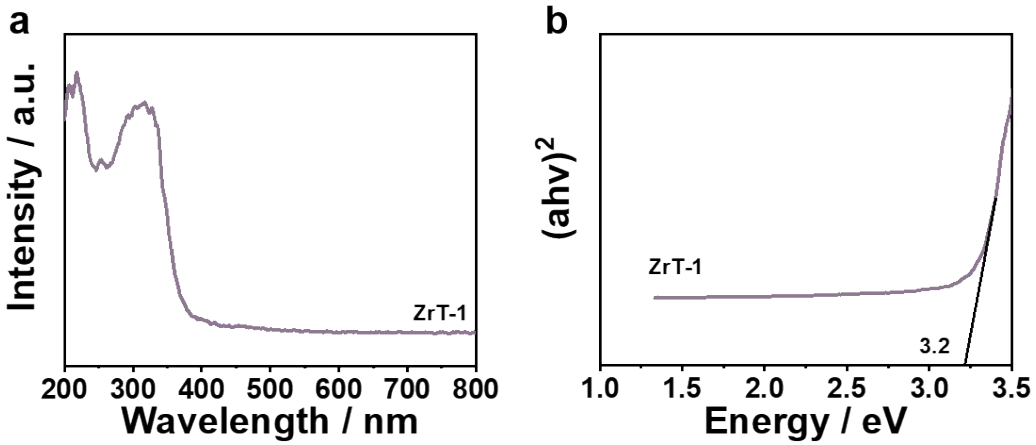

Fig. S11. (a) UV-vis absorption spectrum of ZrT-1. (b) Tauc plot of ZrT-1.

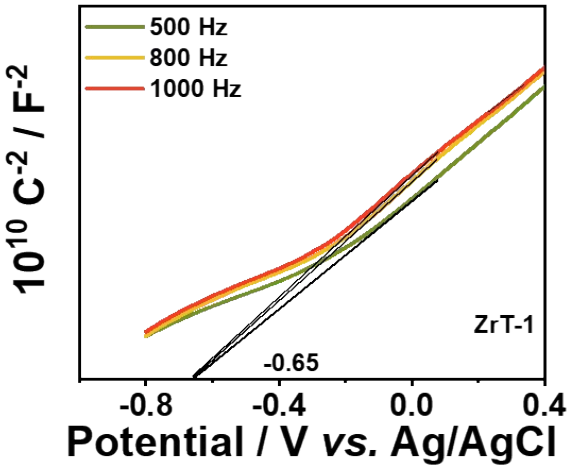

Fig. S12. Mott-Schottky plots of ZrT-1.

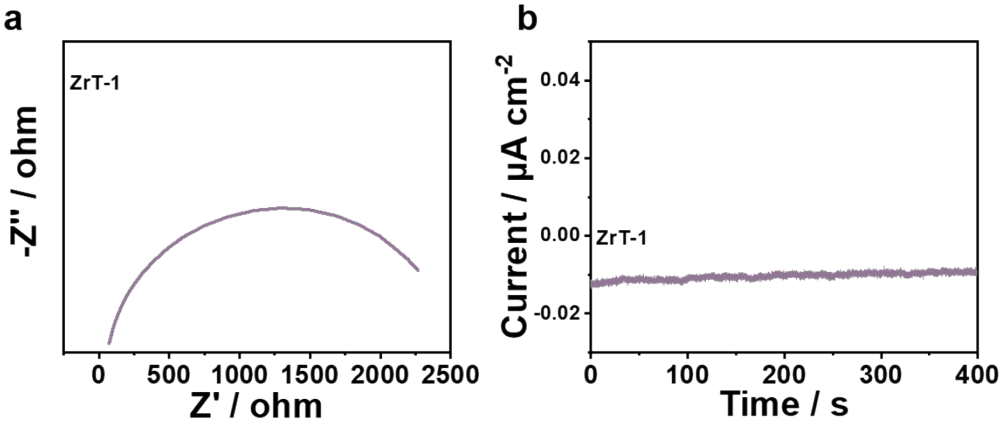

Fig. S13. (a) EIS Nyquist plot of ZrT-1. (b) Transient photocurrent response of ZrT-1.

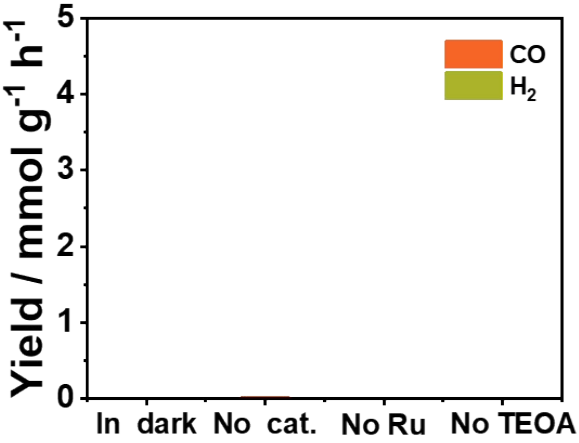

Fig. S14. Photocatalytic performances of Schiff-base ZrOC-1 under different reaction conditions.

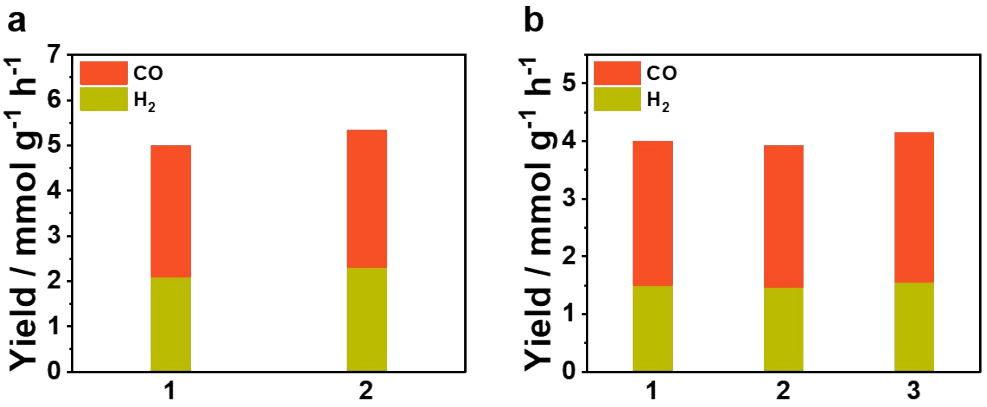

Fig. S15. (a) Yield of reduced product after continued addition of 7 mg $Ru(bpy)_3Cl_2$ to the system. (b) Reproducibility experiments with Schiff-base ZrOC-1.

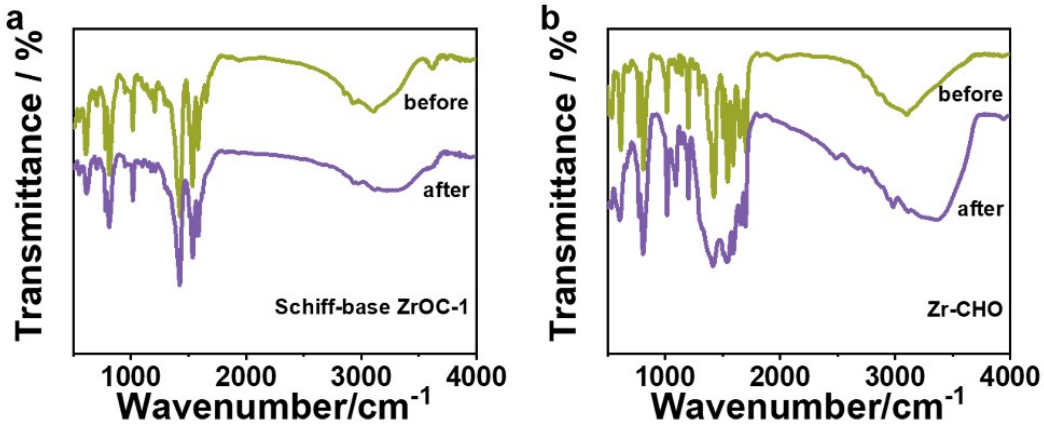

Fig. S16. FT-IR spectra of Schiff-base ZrOC-1 (a) and Zr-CHO (b).

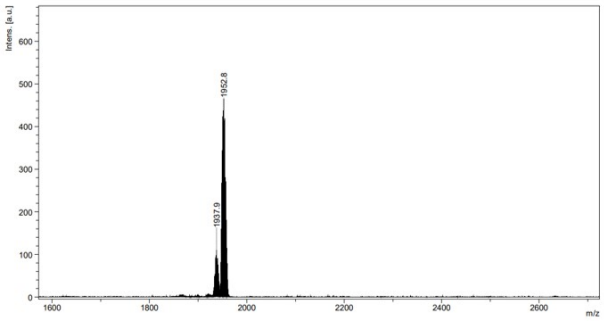

Fig. S17. The MS of Schiff-base ZrOC-1 in TEOA.

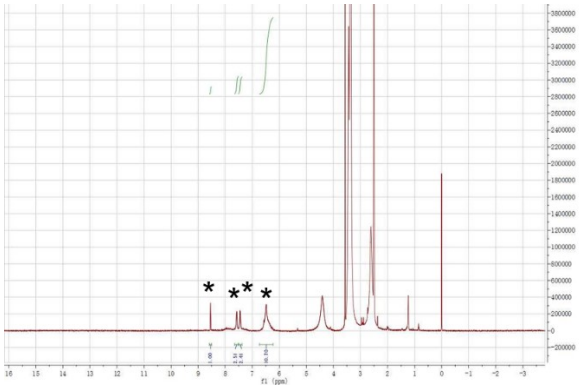

Fig. S18. ^{1}H-NMR spectrum of Schiff-base ZrOC-1 in TEOA.

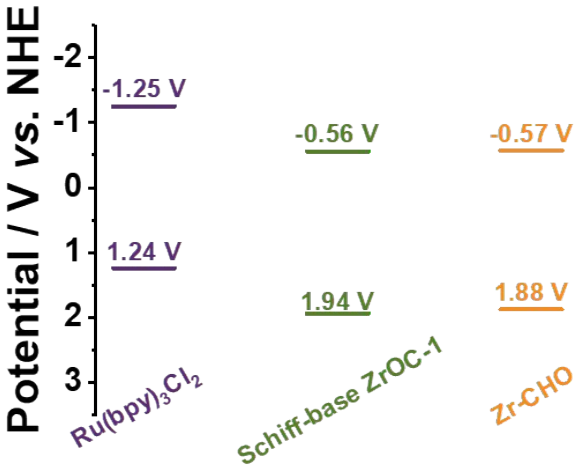

Fig. S19. Band structure diagram for Zr-CHO and Schiff-base ZrOC-1.

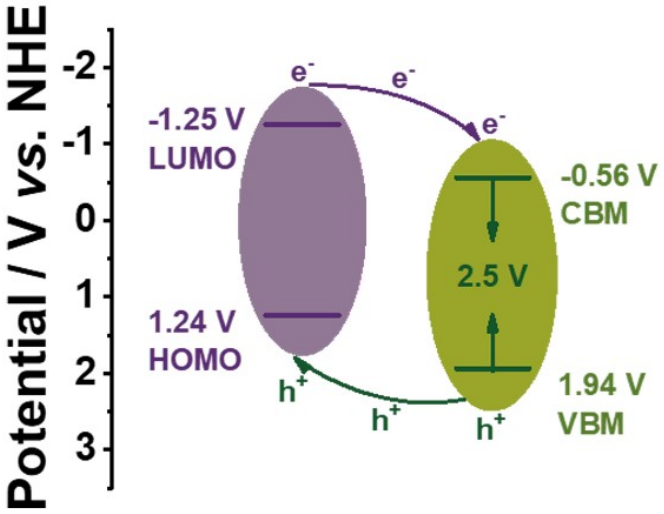

Fig. S20 Possible mechanism of Schiff-base ZrOC-1 for photoreduction of CO_2.